

## Method for the determination of the strength of Brønsted acid sites by adsorption of $^{13}\text{C}$ -2-acetone and $^{13}\text{C}$ CPMAS NMR

**Spectroscopic background:** The  $^{13}\text{C}$  NMR shifts of carbonyl atoms in  $^{13}\text{C}$ -2-acetone dissolved in  $\text{CDCl}_3$  and in a 100 % sulphuric acid solution are  $\delta_{13\text{C}} = 205$  and 245 ppm, respectively [1]. Based on these data and the experimentally determined dependence of the resonance positions of carbonyl atoms in  $^{13}\text{C}$ -2-acetone dissolved in aqueous sulphuric acid with varying concentration, a scale of the Brønsted acid strength was introduced [1] (**Fig. 1, last line**, and Fig. 5, last line, in Ref. [1]) corresponding to a higher acid strength for a higher  $^{13}\text{C}$  chemical shift value of adsorbed  $^{13}\text{C}$ -2-acetone. In **Fig. 1**, the  $^{13}\text{C}$  chemical shift range of  **$^{13}\text{C}$ -2-acetone adsorbed at Brønsted acid sites of zeolites** covers the range of  $\delta_{13\text{C}} = 215$  ppm for zeolite H,Na-X with low acid strength up to  $\delta_{13\text{C}} = 223$  ppm for zeolite H-ZSM-5 with high acid strength.

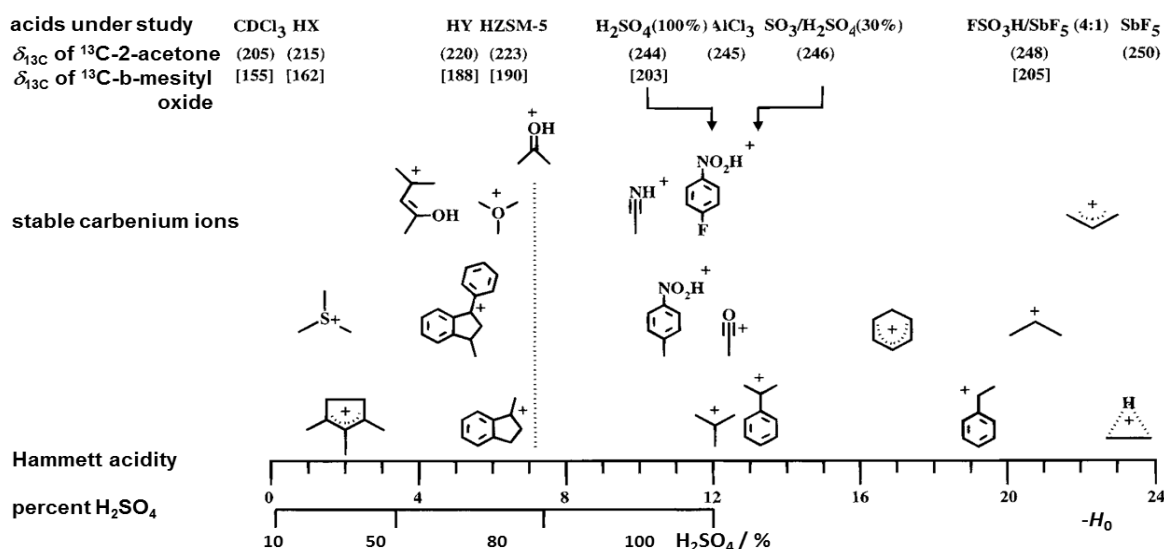


Fig. 1

A number of research groups [1-5] studied various solid catalysts by adsorption of  $^{13}\text{C}$ -2-acetone and obtained the following sequence of the  $^{13}\text{C}$  chemical shifts of the carbonyl atoms corresponding to an increasing Brønsted acid strength of these materials:

**Silica ( $\delta_{13\text{C}} = 210.0$  ppm [2]) < H-SAPO-5 ( $\delta_{13\text{C}} = 216.8$  ppm [3]) < H-SAPO-34 ( $\delta_{13\text{C}} = 217.0$  ppm [4]) < H,Na-Y ( $\delta_{13\text{C}} = 219.6$  ppm [3]) < H-MOR ( $\delta_{13\text{C}} = 221.8$  ppm [3]) < H-[Ga]ZSM-5 ( $\delta_{13\text{C}} = 222.8$  ppm [3]) < H-ZSM-12 ( $\delta_{13\text{C}} = 223.4$  ppm [3]) < H-ZSM-5**

( $\delta_{13\text{C}} = 223.6 \text{ ppm}$  [3]) < H-ZSM-33 ( $\delta_{13\text{C}} = 225.4 \text{ ppm}$  [3]) <  $\text{H}_3\text{PW}_{12}\text{O}_{40}$  and  $\text{AIPW}_{12}\text{O}_{40}$  ( $\delta_{13\text{C}} = 235 \text{ ppm}$  [5]).

Based on the  $^{13}\text{C}$  CPMAS NMR spectra of aluminum-modified Na- and H-ZSM-5 zeolites in **Fig. 2**, the following sequence of the Brønsted acid strength was found [6]:

**Al/Na-ZSM-5/1** ( $\delta_{13\text{C}} = 218 + \text{weak } 223 \text{ ppm}$ ) < **Al/NaZSM-5/2** ( $\delta_{13\text{C}} = 218 + 223 \text{ ppm}$ ) < **H-ZSM-5** ( $\delta_{13\text{C}} = 223 \text{ ppm}$ ) < **Al/H-ZSM-5/1** ( $\delta_{13\text{C}} = \text{weak } 218 + 223 + \text{weak } 225 \text{ ppm}$ ) < **Al/H-ZSM-5/2** ( $\delta_{13\text{C}} = 225 + \text{weak } 228 \text{ ppm}$ )

In **Fig. 2**, the  $^{13}\text{C}$  CPMAS NMR signals at  $\delta_{13\text{C}} = 210 \text{ ppm}$  are due to  $^{13}\text{C}$ -2-acetone adsorbed at SiOH groups, while signals at  $\delta_{13\text{C}} \approx 235 \text{ ppm}$  are caused by Lewis acid sites due to extra-framework aluminum. These aluminum species inside zeolite pores enhance the acid strength of the Brønsted sites in their vicinity. According to the above-mentioned sequence, aluminum-modified H-ZSM-5 zeolites have a higher acid strength than aluminum-modified Na-ZSM-5 zeolites. The Al/H-ZSM-5 catalysts are at the upper limit of the Brønsted acid strength of zeolites and, therefore, also of the  $^{13}\text{C}$  chemical shift range of  $^{13}\text{C}$ -2-acetone adsorbed on Brønsted acidic zeolites.

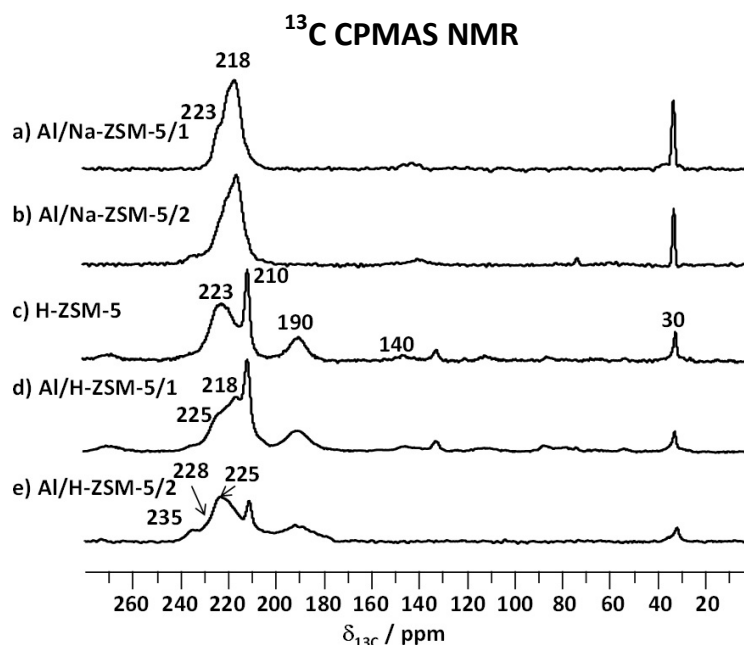


**Fig. 2**

Similarly, the Brønsted acid strength of flame-derived silica-zirconia (SZ/x with  $x = 100$  means pure zirconia), prepared by flame-spray pyrolysis (FSP), was investigated

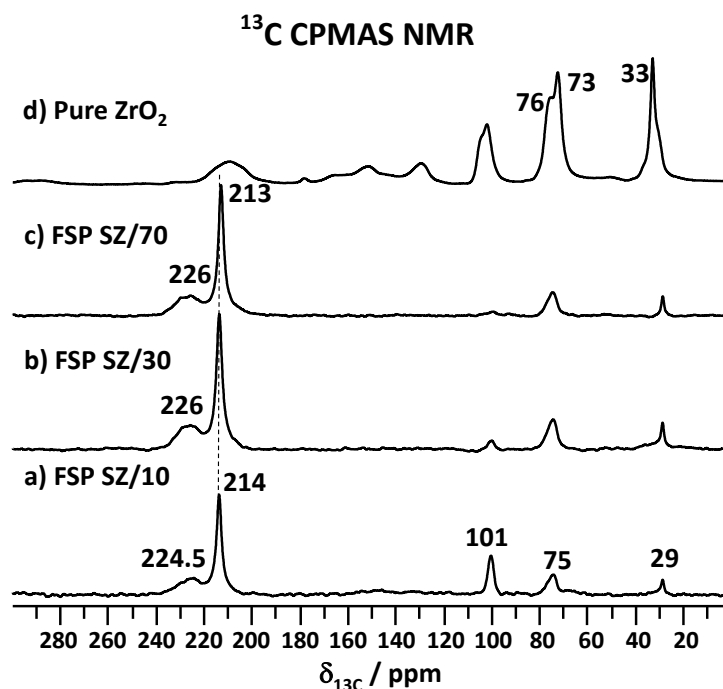


Fig. 3

by adsorption of <sup>13</sup>C-2-acetone and <sup>13</sup>C CPMAS NMR spectroscopy (see **Fig. 3**) [7]. Signals at  $\delta_{13C} = 226$  ppm for SZ/x samples with  $x = 30$  and  $70$  hint at the presence of Brønsted acid sites with an acid strength comparable with that of the strongest zeolites (compare with **Fig. 2**). The signals at  $\delta_{13C} = 73$  to  $76$  ppm in the <sup>13</sup>C MAS NMR spectrum of **Fig. 3d** are caused by the products of an aldol reaction of the <sup>13</sup>C-2-acetone at strong Lewis acid sites of pure ZrO<sub>2</sub>. For studies on the application of <sup>13</sup>C-2-acetone as molecular probe molecules for Lewis sites on solid catalysts, see Section “method 24” and Refs. [8], [9], and [10].

**Catalyst preparation:** Before the <sup>13</sup>C CPMAS NMR studies, a standard dehydration of the solid catalyst inside a “sample tube system 1” at “vacuum line 1” (see Sections “sample tube system 1” and “vacuum line 1”, accessible via link “*In Situ* Solid-State NMR Techniques”) was performed. The dehydration starts with an evacuation at room temperature for ca. 10 minutes followed by a temperature ramp from room temperature to  $T = 393$  K within 2 hours. At this temperature, the sample was dehydrated for 2 hours. Subsequently, the temperature was increased up to  $T = 723$  K within 3 hours and the sample was evacuated at this temperature for 12 hours.

After this treatment, the sample tube system was closed via the vacuum valve and disconnected from „vacuum line 1“ (after this line was ventilated with air).

Subsequently, the sample tube system with the dehydrated catalyst and the vessel with  $^{13}\text{C}$ -2-acetone were connected at “vacuum line 2” as shown in Fig. 7 of the Section “vacuum line 2”, accessible via link “*In Situ* Solid-State NMR Techniques”. If the  $^{13}\text{C}$ -2-acetone (99.5%, SIGMA-ALDRICH) is used for the first time, gas impurities were removed by thrice freezing and evacuation. For this purpose the  $^{13}\text{C}$ -2-acetone vessel was put into a dewar with liquid nitrogen. After the acetone becomes rigid, open the valve of the vessel for an evacuation of the gas inside and close this valve again. Upon an evacuation of the line for ca. 10 minutes, close the valve connecting the vacuum line with the pump (large left valve). Now, open the valve of the acetone vessel until an acetone pressure of ca. 50 mbar is reached in the vacuum line and close the valve of the vessel. Put the lower part of the sample tube into a dewar filled liquid nitrogen and open the valve of this sample tube system. During acetone adsorption, warm up the catalyst sample by hand to room temperature and wait 10 minutes for better distribution of the molecules in the sample. Subsequently, slowly open the left valve of the “vacuum line 2” to the pump and evacuate the sample tube for 10 minutes at room temperature for the removal of surplus molecules. For the removal of the acetone from SiOH and AlOH groups, the evacuation time can be 2 to 10 hours. Close the valve of the sample tube system and disconnect it from the vacuum line (after this line was ventilated by air).

**$^{13}\text{C}$  MAS NMR studies:** The  $^{13}\text{C}$ -2-acetone-loaded catalyst in the sample tube system was transferred into an MAS NMR rotor without air contact inside a mini glove box (see Section “mini glove box”, accessible via link “*In Situ* Solid-State NMR Techniques”), purged with dry nitrogen gas, and, finally, the rotor was sealed with a gas-tight rotor cap. All above-mentioned  $^{13}\text{C}$  cross-polarization (CP) MAS NMR spectra were recorded at a Bruker AVANCE III 400 WB spectrometer with a  $^{13}\text{C}$  resonance frequency of  $\nu_0 = 100.6$  MHz, using a 4 mm MAS NMR probe with a sample spinning rate of 8 kHz, a contact time of 4 ms, and a repetition time of 4 s. For decreasing the  $^{13}\text{C}$  CPMAS NMR line width, high-power  $^1\text{H}$  decoupling was applied during recording the induction decay of  $^{13}\text{C}$  spins. Chemical shifts were referenced to adamantane powder ( $\delta_{13\text{C}} = 38.55$  and 29.50 ppm) at spinning rates of

$\nu_{\text{rot}} = 2$  to 3 kHz. This reference is easier to handle in MAS NMR rotors than liquid tetramethylsilane (TMS,  $\delta_{13\text{C}} = 0$  ppm) with a boiling point of 299 to 301 K.

### References:

- [1] J.F. Haw, J.B. Nicholas, T. Xu, L.W. Beck, D.B. Ferguson, *Physical organic chemistry of solid acids: Lessons from in situ NMR and theoretical chemistry*, Acc. Chem. Res. 29 (1996) 259-267, DOI: 10.1021/ar950105k.
- [2] J. Huang, N. van Vegten, Y. Jiang, M. Hunger, A. Baiker, *Increasing the Brønsted acidity of flame-derived silica-alumina up to zeolitic strength*, Angew. Chem. Int. Ed. 49 (2010) 7776-7781, DOI: 10.1002/anie.201003391.
- [3] A.I. Biaglow, R.J. Gorte, G.T. Kokotailo, D. White, *A probe of Brønsted site acidity in zeolites –  $^{13}\text{C}$  chemical shift of acetone*, J. Catal. 148 (1994) 779-786, DOI: 10.1006/jcat.1994.1264.
- [4] W. Song, J.B. Nicholas, J.F. Haw, *A persistent carbenium ion on the methanol-to-olefin catalyst HSAPO-34: Acetone shows the way*, J. Phys. Chem. B 105 (2001) 4317-4323, DOI: 10.1021/jp0041407.
- [5] U. Filek, A. Bressel, B. Sulikowski, M. Hunger, *Structural stability and Brønsted acidity of thermally treated AIPW $_{12}\text{O}_{40}$  in comparison with H $_3$ PW $_{12}\text{O}_{40}$* , J. Phys. Chem. C 112 (2008) 19470-19476, DOI: 10.1021/jp807947v.
- [6] Z. Wang, L. Wang, Y. Jiang, M. Hunger, J. Huang, *Cooperativity of Brønsted and Lewis acid sites on zeolite for glycerol dehydration*, ACS Catal. 4 (2014) 1144-1147, DOI: 10.1021/cs401225k.
- [7] Z. Wang, Y. Jiang, M. Hunger, A. Baiker, J. Huang, *Catalytic performance of Brønsted and Lewis acid sites in phenylglyoxal conversion on flame-derived silica-zirconia*, ChemCatChem 6 (2014) 2970-2975, DOI: 10.1002/cctc.201402397.
- [8] Y. Jiang, J. Huang, W. Dai, M. Hunger, *Solid-state nuclear magnetic resonance investigations of the nature, property, and activity of acid sites on solid catalysts*, Solid State Nucl. Magn. Reson. 39 (2011) 116-141, DOI: 10.1016/j.ssnmr.2011.03.007.
- [9] W. Yang, Z. Wang, J. Huang, Y. Jiang, *Qualitative and Quantitative Analysis of Acid Properties for Solid Acids by Solid-State Nuclear Magnetic Resonance Spectroscopy*, J. Phys. Chem. C 125(19) (2021) 10179-10197, DOI: 10.1021/acs.jpcc.1c01887.
- [10] M. Dyballa, *Solid-State NMR Probe Molecules for Catalysts and Adsorbents: Concepts, Quantification, Accessibility, and Spatial Distribution*, Energy & Fuels 37(23) (2023) 18517-18559, DOI: 10.1021/acs.energyfuels.3c03815.